Modeling, Testing and Calibration of Ductile Fracture

Lab facility

Custom-made biaxial testing machine

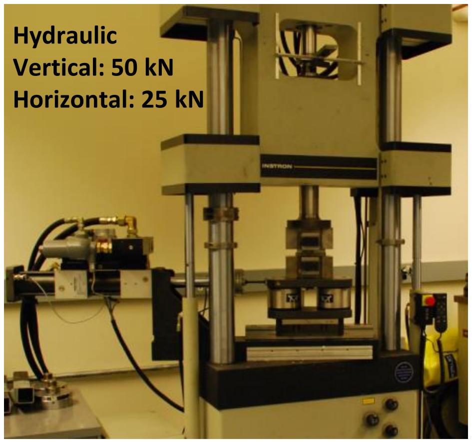

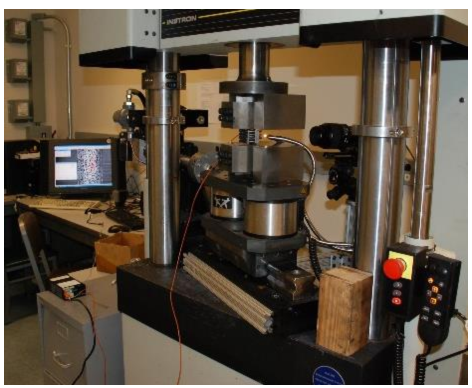

Tension–compression test

MTS universal testing machine

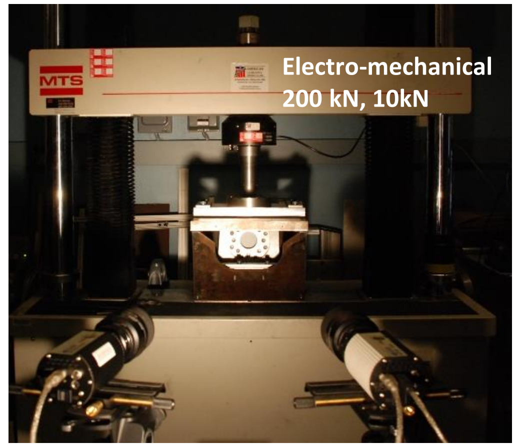

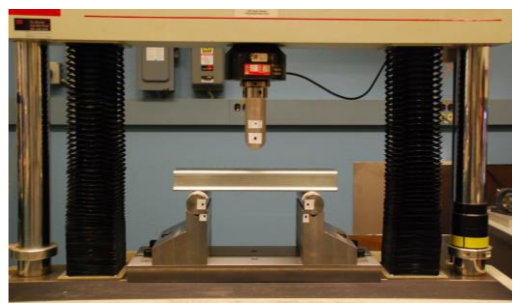

Three-point bending of a hat assembly

SHPB systems in France

INSTRON 9250HV

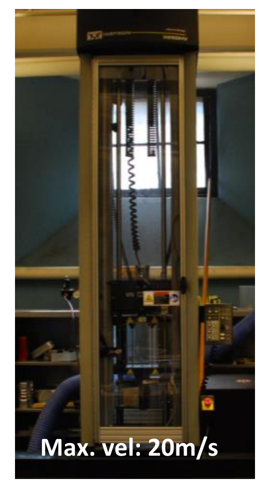

INSTRON 5944

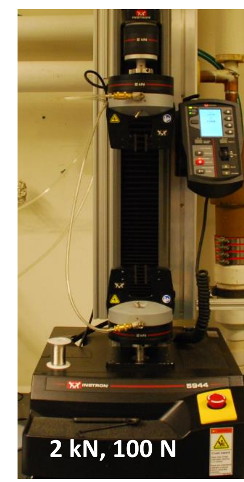

Vic 2D and Vic 3D software, two digital cameras, high speed cameras, Abaqus, LS-DYNA, Hypermesh, workstations

Plasticity

Conventional metal plasticity

* Yield surface

- Von Mises yield criterion: $f(\boldsymbol{\sigma},\bar{\varepsilon}_p)=\sqrt{\frac{3}{2}\boldsymbol{\sigma}':\boldsymbol{\sigma}'}-k(\bar{\varepsilon}_p)\le 0$

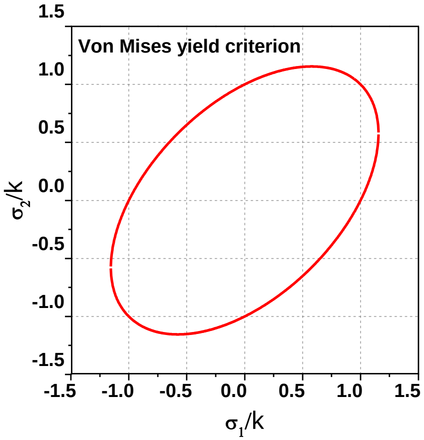

* Flow rule

- Associated flow rule: $d\boldsymbol{\varepsilon}_p = d\bar{\varepsilon}_p \frac{\partial f}{\partial \boldsymbol{\sigma}}$

(Plastic potential=yield function)

* Hardening law

- Swift law: $k(\bar{\varepsilon}_p)=A(\varepsilon_0+\bar{\varepsilon}_p)^n$
- Voce law: $k(\bar{\varepsilon}_p)=k_0+Q(1-\exp(-\beta\bar{\varepsilon}_p))$
- Extrapolation up to a large strain
- Isotropic hardening

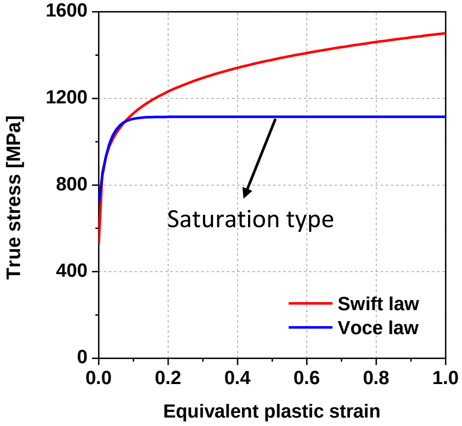

Anisotropy and non-associated flow rule*

* Different anisotropy between yield stress and Lankford ratio (r-value), $r_\alpha = \dfrac{d\varepsilon_w}{d\varepsilon_t}$

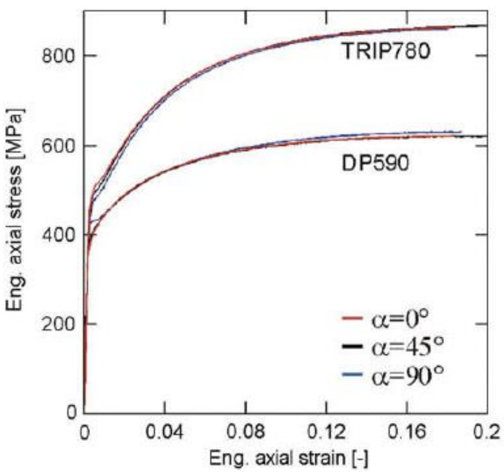

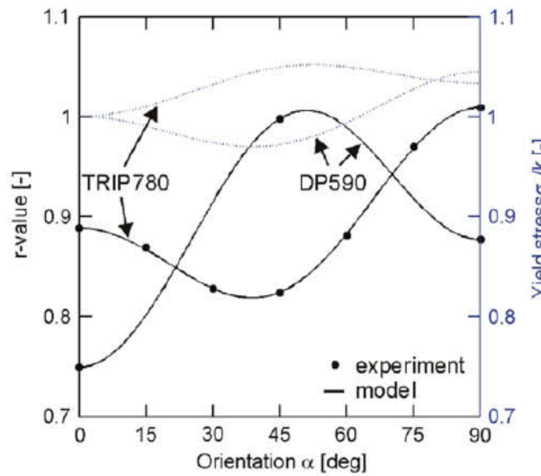

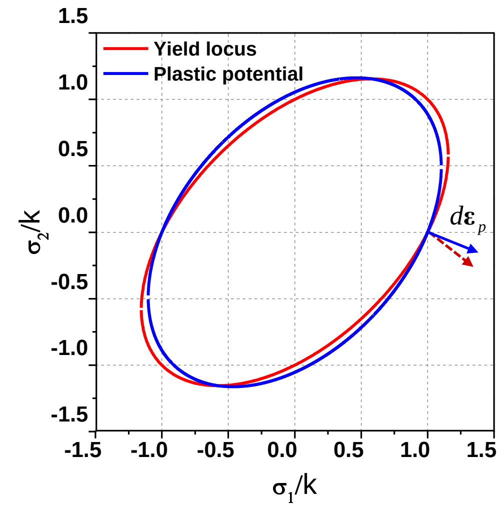

Non-associated flow rule

$$f(\boldsymbol{\sigma}, \bar{\varepsilon}_p) = \sqrt{(\mathbf{P}\boldsymbol{\sigma})\cdot\boldsymbol{\sigma}} - k(\bar{\varepsilon}_p) \le 0$$

$$g(\boldsymbol{\sigma}) = \sqrt{(\mathbf{G}\boldsymbol{\sigma})\cdot\boldsymbol{\sigma}} \Rightarrow d\boldsymbol{\varepsilon}_p = d\lambda \frac{\partial g}{\partial \boldsymbol{\sigma}}$$

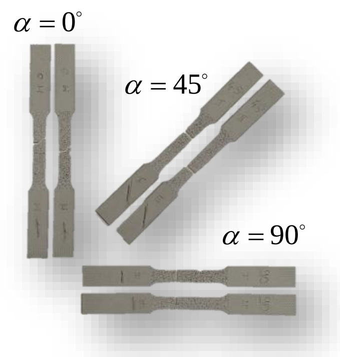

Associated flow rule

$$f(\boldsymbol{\sigma}, \bar{\varepsilon}_p) = \sqrt{(\mathbf{P}\boldsymbol{\sigma})\cdot\boldsymbol{\sigma}} - k(\bar{\varepsilon}_p) \le 0$$

$$d\boldsymbol{\varepsilon}_p = d\bar{\varepsilon}_p \frac{\partial f}{\partial \boldsymbol{\sigma}}$$

*Mohr et al. "Evaluation of associated and non-associated quadratic plasticity models for advanced high strength steel sheets under multi-axial loading, International Journal of Plasticity, Vol. 26, pp. 939-956, 2010.

Validation of non-associated flow rule

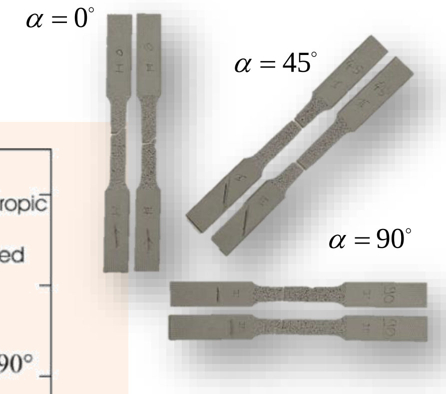

* Validation with DP590 and TRIP780

DP 590

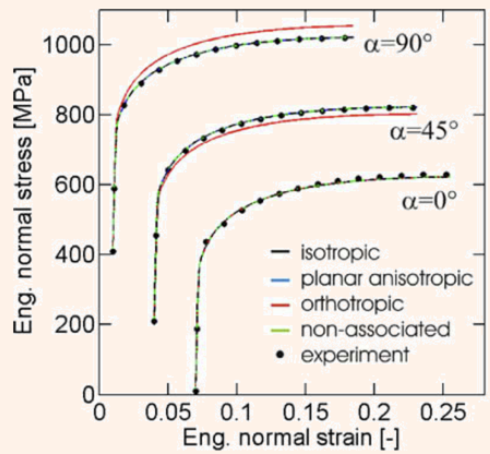

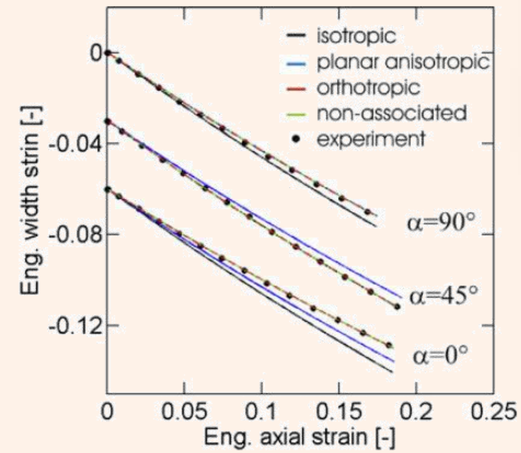

TRIP 780

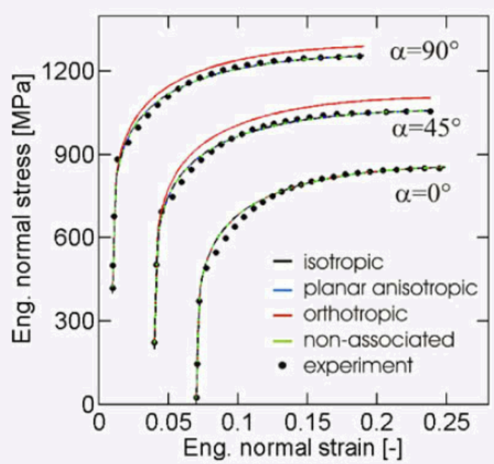

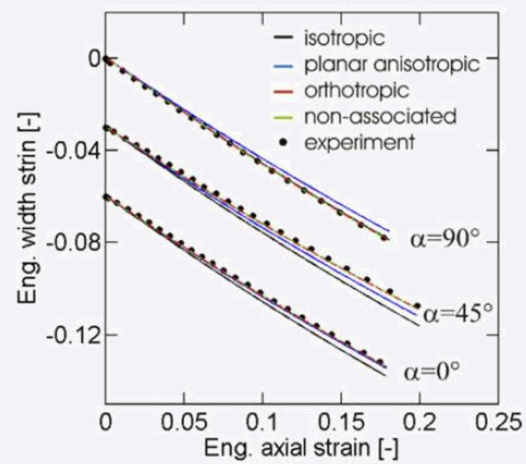

Hardening curve after necking

* Fracture occurs after a significant amount of necking
- Need for the stress−strain curve after necking
- Non-uniform deformation in the gauge section after necking
  → hard to obtain hardening curve after necking experimentally

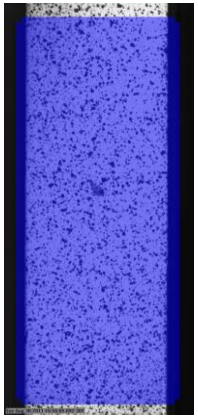

* 'Inverse method' using finite element simulation
- Use of so-called 'Notch tension test' with R20 mm
- Adjustment to the stress−strain curve in the post necking area until force −displacement curve from simulation agrees well with the one from the experiment
- It is unavoidable to repeat simulation

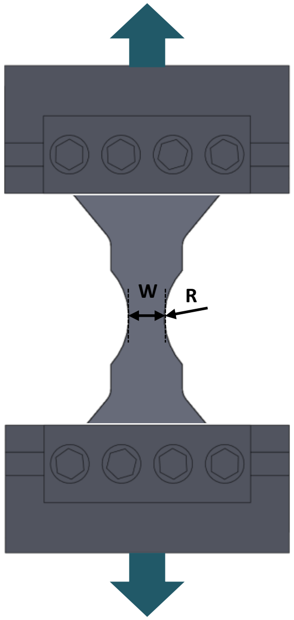

* Why 'Notch tension test'?
- Its geometry always generates necking exactly in the middle of specimen because of the minimum gauge width there
- Robustness and repeatability of tests

Procedure for inverse method

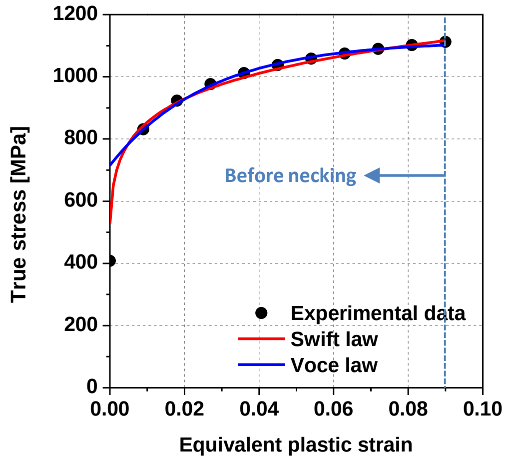

$$k_{Swift}(\bar{\varepsilon}_p) = A(\varepsilon_0 + \bar{\varepsilon}_p)^n$$

$$k_{Voce}(\bar{\varepsilon}_p) = k_0 + Q(1 - \exp(-\beta \bar{\varepsilon}_p))$$

A	1501
ε_0	0.0002
n	0.123
k_0	715
Q	400
β	37.9

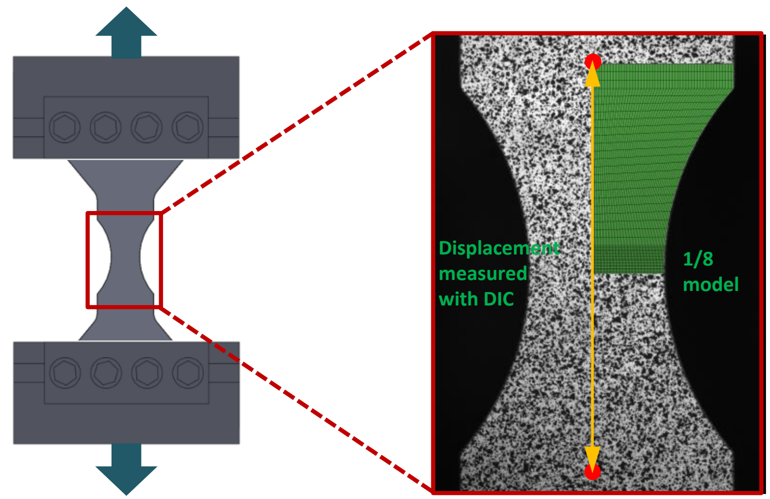

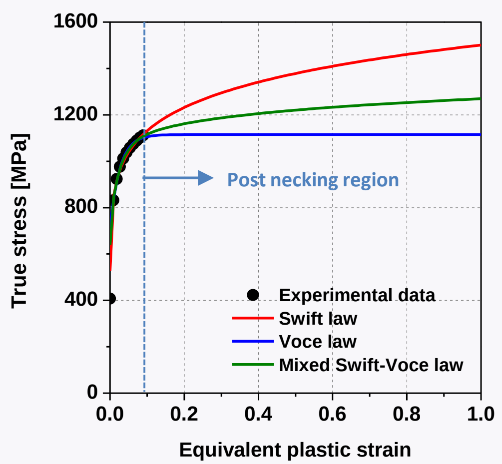

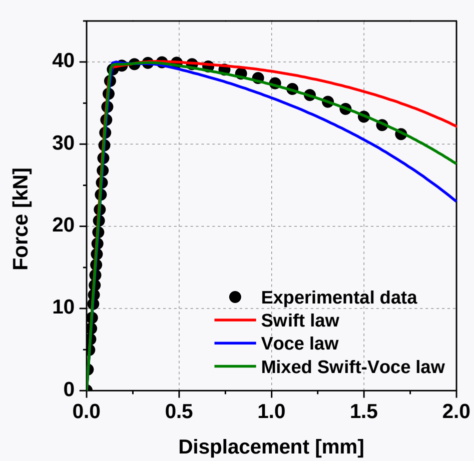

Mixed Swift−Voce law

$$k(\bar{\varepsilon}_p) = \alpha k_{Swift}(\bar{\varepsilon}_p) + (1-\alpha) k_{Voce}(\bar{\varepsilon}_p)$$

α : weighting factor

Strain rate dependency*

* Rate dependent hardening model

$$k[\bar{\varepsilon}_p, \dot{\bar{\varepsilon}}_p, T] = k_\varepsilon[\bar{\varepsilon}_p]\, k_{\dot{\varepsilon}}[\dot{\bar{\varepsilon}}_p]\, k_T[T]$$

$$k(\bar{\varepsilon}_p) = \alpha k_{Swift}(\bar{\varepsilon}_p) + (1-\alpha) k_{Voce}(\bar{\varepsilon}_p)$$

$$k_{\dot{\varepsilon}}[\dot{\bar{\varepsilon}}_p] = \begin{cases} 1 & \text{for } \dot{\bar{\varepsilon}}_p < \dot{\varepsilon}_0 \\ 1 + C \ln\left[\dfrac{\dot{\bar{\varepsilon}}_p}{\dot{\varepsilon}_0}\right] & \text{for } \dot{\bar{\varepsilon}}_p \geq \dot{\varepsilon}_0 \end{cases}$$

$$k_T[T] = \begin{cases} 1 & \text{for } T < T_r \\ 1 - \left(\dfrac{T - T_r}{T_m - T_r}\right)^m & \text{for } T_r \leq T \leq T_m \end{cases}$$

$$dT = w[\dot{\bar{\varepsilon}}_p] \frac{\eta_k}{\rho C_p} \bar{\sigma} d\bar{\varepsilon}_p \quad (\eta_k : \text{Taylor-Quinney coefficient})$$

$$w[\dot{\bar{\varepsilon}}_p] = \begin{cases} 0 & \text{for } \dot{\bar{\varepsilon}}_p < \dot{\varepsilon}_{it} \\ \dfrac{(\dot{\bar{\varepsilon}}_p - \dot{\varepsilon}_{it})^2 (3\dot{\varepsilon}_a - 2\dot{\bar{\varepsilon}}_p - \dot{\varepsilon}_{it})}{(\dot{\varepsilon}_a - \dot{\varepsilon}_{it})^3} & \text{for } \dot{\varepsilon}_{it} \leq \dot{\bar{\varepsilon}}_p \leq \dot{\varepsilon}_a \\ 1 & \text{for } \dot{\bar{\varepsilon}}_a < \dot{\varepsilon}_{it} \end{cases}$$

Experimental setup

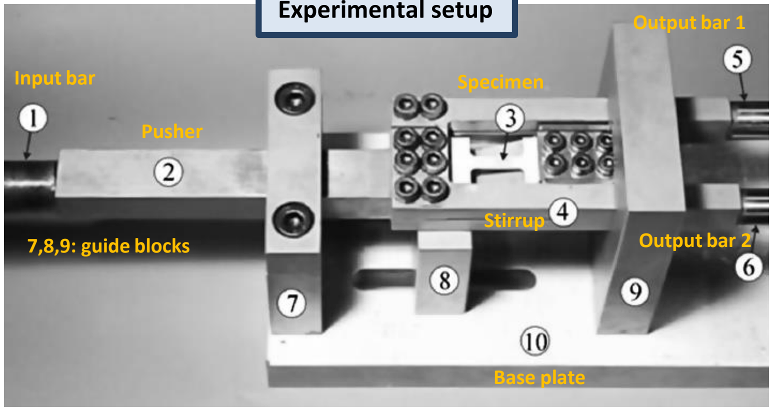

Dependency of weighting factor on strain rate

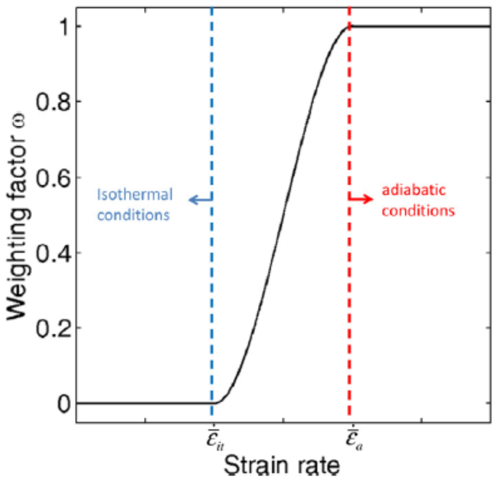

*Roth and Mohr, "Effect of strain rate on ductile fracture initiation in advanced high strength steel sheets: Experiments and modeling", International Journal of Plasticity, Vol. 56, pp. 19-44, 2014

Plasticity model for reverse loading (MYU)

* Plasticity model for reverse loading **(by Stephane Marcadet)**

- Compression followed by tension or tension followed by compression
- New behaviors should be incorporated into plasticity model
  - Bauschinger effect
  - Work hardening stagnation
  - Permanent softening
- Kinematic hardening is used instead of isotropic hardening
- Four parameters $[\gamma,\ \eta,\ \phi,\ \beta]$
- Calibration of the model based on uniaxial tension followed by compression
- Effect of four parameters

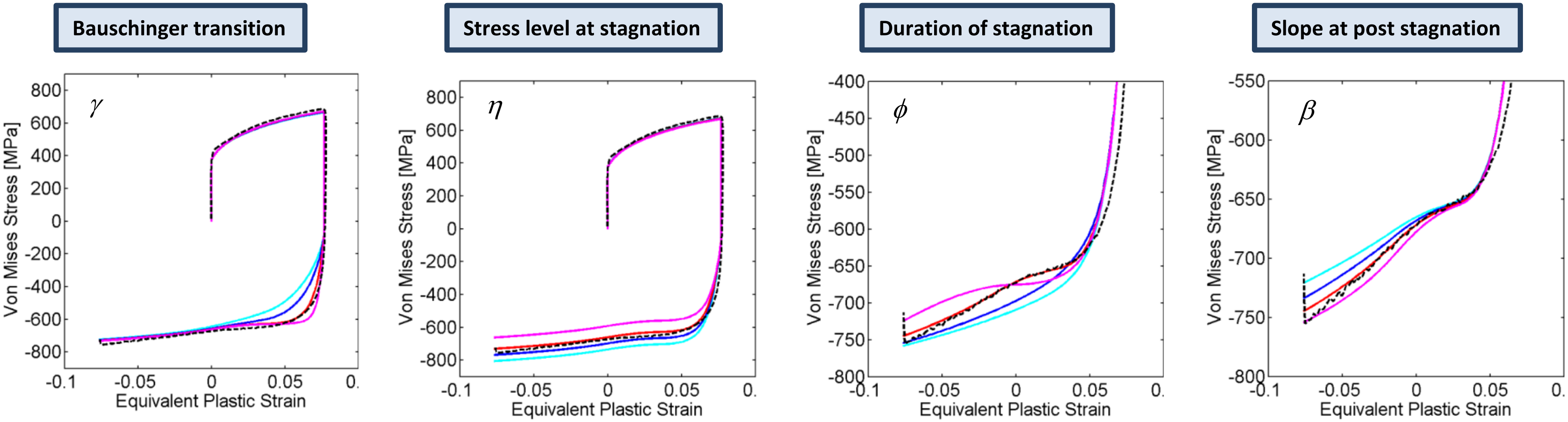

Novel experiment technique for plasticity

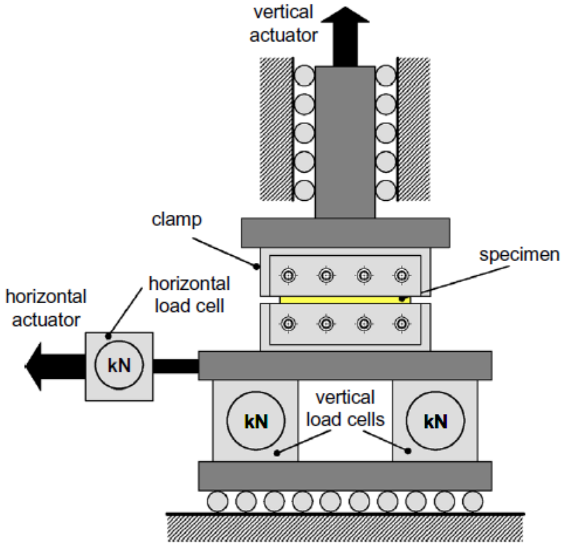

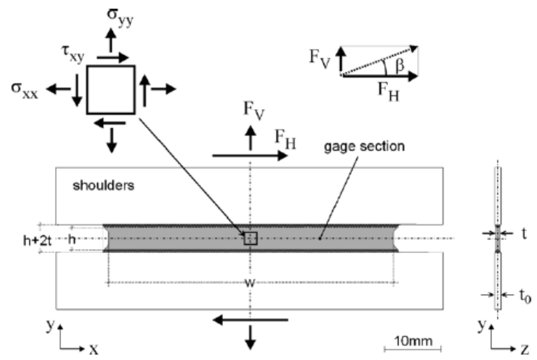

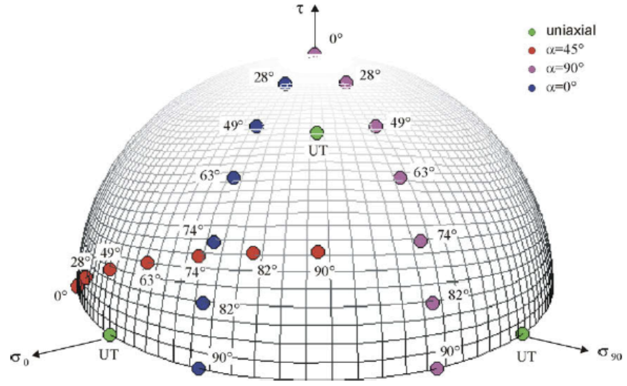

Fracture model

Loading path parameter

* Formulation of stress triaxiality η and Lode angle $\bar{\theta}$

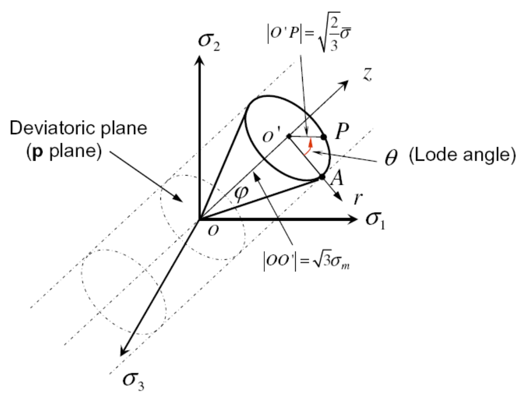

<Principal stress space>

$\overrightarrow{OP} = (\sigma_1, \sigma_2, \sigma_3)$ Load vector in Cartesian coord.

$\overrightarrow{OO'} = (\sigma_m, \sigma_m, \sigma_m)$ Hydrostatic pressure vector

$\overrightarrow{O'P} = (\sigma_1 - \sigma_m, \sigma_2 - \sigma_m, \sigma_3 - \sigma_m) = (s_1, s_2, s_3)$

$$\left|\overrightarrow{O'P}\right| = \sqrt{s_1^2 + s_2^2 + s_3^2} = \sqrt{2J_2} = \sqrt{\frac{2}{3}}\bar{\sigma}_{Mises}$$

$$\theta = \frac{1}{3}\cos^{-1}\left(\frac{27\det[s_{ij}]}{2\bar{\sigma}_{Mises}^3}\right)$$

$\therefore$ Cartesian coord. $\rightarrow$ Cylindrical coord. (Haigh-Westergaard coord.)

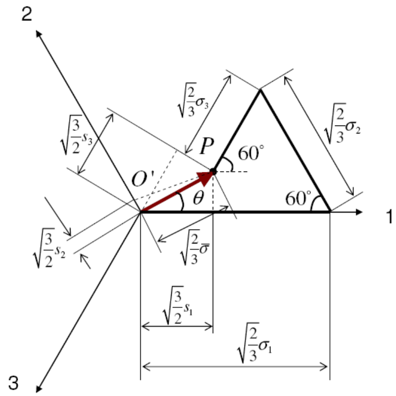

<Deviatoric π-plane>

$$\eta = \frac{-p}{\bar{\sigma}} = \frac{\sigma_m}{\bar{\sigma}} = \frac{\sqrt{2}}{3}\cot\varphi, \quad (\eta : \text{Stress triaxiality})$$

$$\bar{\theta} = 1 - \frac{6\theta}{\pi}, \quad (\bar{\theta} : \text{Normalized Lode angle, } 0^\circ \le \theta \le 60^\circ)$$

$(\eta,\ \bar{\theta})$: Representing specific loading path

History of fracture models at ICL

Three-branch fracture model[(1)]

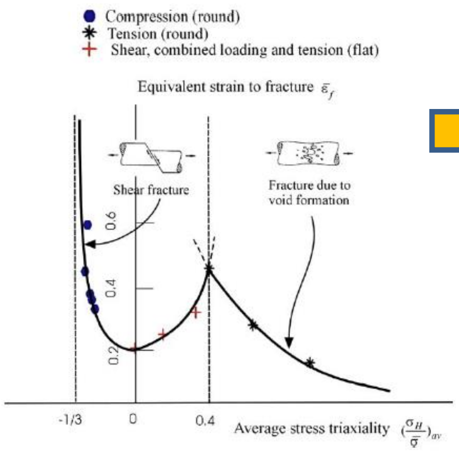

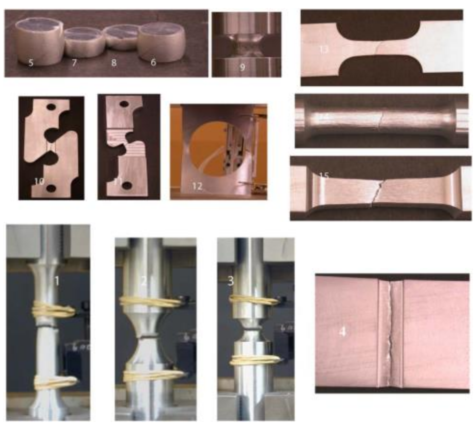

Modified Mohr–Coulomb model (2010)[(2)]

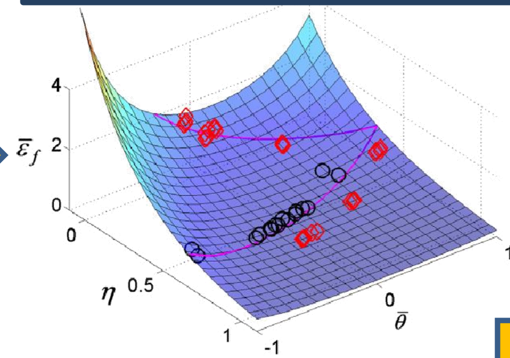

$$\hat{\varepsilon}_p^f = \left\{\frac{A}{c_2}\left[c_3 + \frac{\sqrt{3}}{2-\sqrt{3}}(1-c_3)\left(\sec\left(\frac{\bar{\theta}\pi}{6}\right)-1\right)\right]\left[\sqrt{\frac{1+c_1^2}{3}}\cos\left(\frac{\bar{\theta}\pi}{6}\right)+c_1\left(\eta+\frac{1}{3}\sin\left(\frac{\bar{\theta}\pi}{6}\right)\right)\right]\right\}^{-\frac{1}{n}}$$

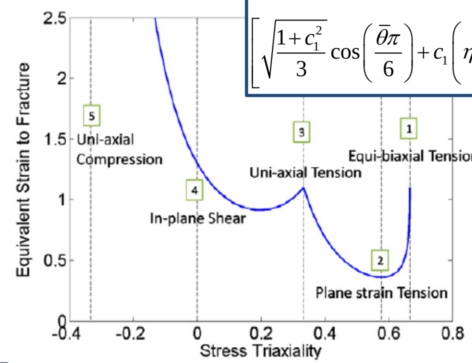

$$D = \int_0^{\bar{\varepsilon}_p^f} \frac{d\bar{\varepsilon}_p}{\hat{\varepsilon}_p^f(\eta,\bar{\theta})}$$

Extended Mohr–Coulomb model (2014)[(3), (4)]

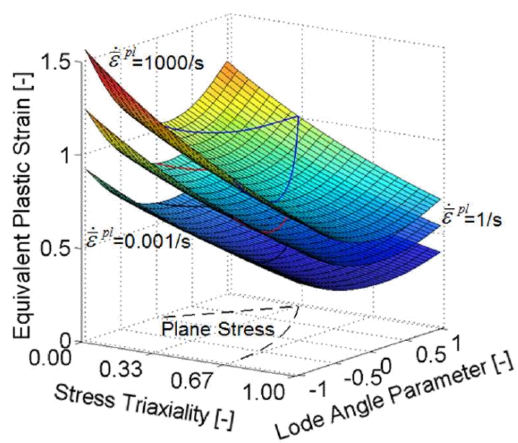

$$\hat{\varepsilon}_p^f(\eta,\bar{\theta}) = b(1+c)^{\frac{1}{n}}\left[\left\{\frac{1}{2}\left((f_1-f_2)^a+((f_2-f_3)^a+(f_3-f_1)^a\right)^{\frac{1}{a}}\right\} + c\left(2\eta+f_1+f_3\right)\right]^{-\frac{1}{n}}$$

$$b = \begin{cases} b_0 & \text{for } \dot{\bar{\varepsilon}}_p < \dot{\varepsilon}_0 \\ b_0\left(1+\gamma\ln\left[\frac{\dot{\bar{\varepsilon}}_p}{\dot{\varepsilon}_0}\right]\right) & \text{for } \dot{\bar{\varepsilon}}_p \geq \dot{\varepsilon}_0 \end{cases}$$

(1) Bao and Wierzbicki, "On fracture locus in the equivalent strain and stress triaxiality space", International Journal of Mechanical Sciences, Vol. 46, pp. 81-98, 2004.
(2) Bai and Wierzbicki, "Application of extended Mohr–Coulomb criterion to ductile fracture", International Journal of Fracture, Vol. 161, pp. 1-20, 2010.
(3) Mohr and Marcadet, "Hosford–Coulomb model for predicting the onset of ductile fracture at low stress triaxialities", submitted for the publication.
(4) Roth and Mohr, "Effect of strain rate on ductile fracture initiation in advanced high strength steel sheets: Experiments and modeling", International Journal of Plasticity, Vol. 56, pp. 19-44, 2014.

Calibration of fracture model

* Fracture tests

5 types of tests characterizing a different combination of $\bar{\theta}$ and η

- NTR 20: notch tension with R20
- NTR 6: notch tension with R6
- CHD4: central hole with D4
- Butterfly: tension & shear (plane strain tension & pure shear)
- Punch: biaxial tension

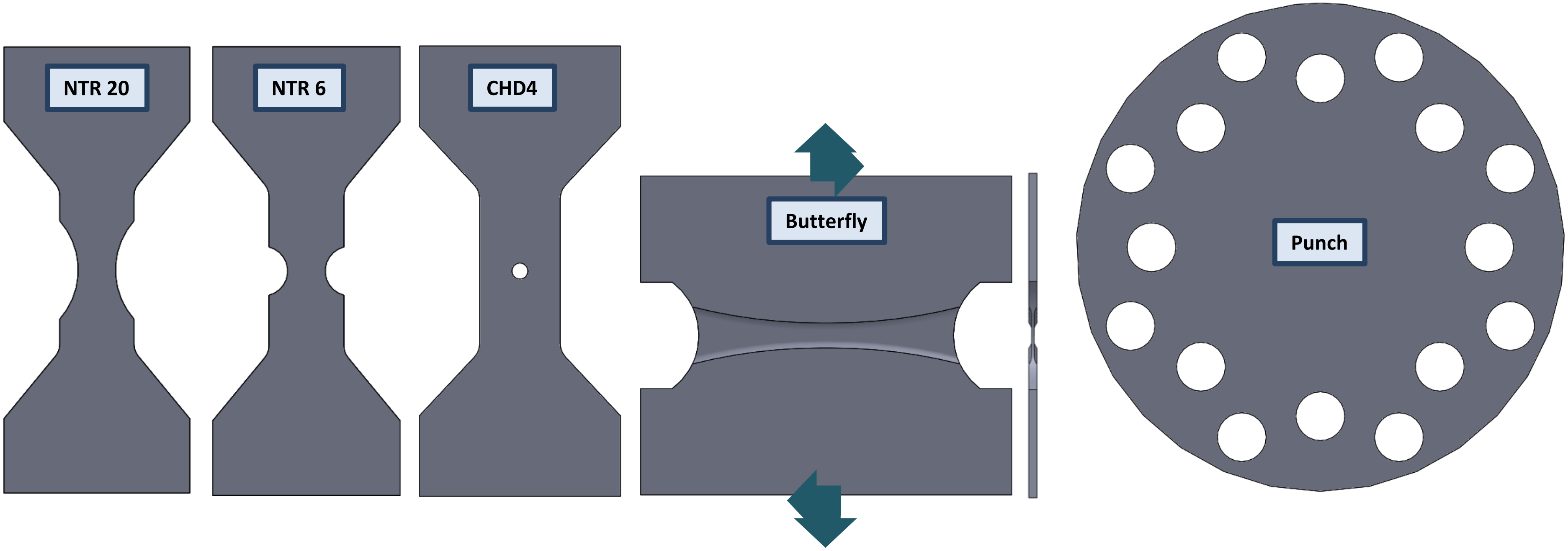

Identification of loading path

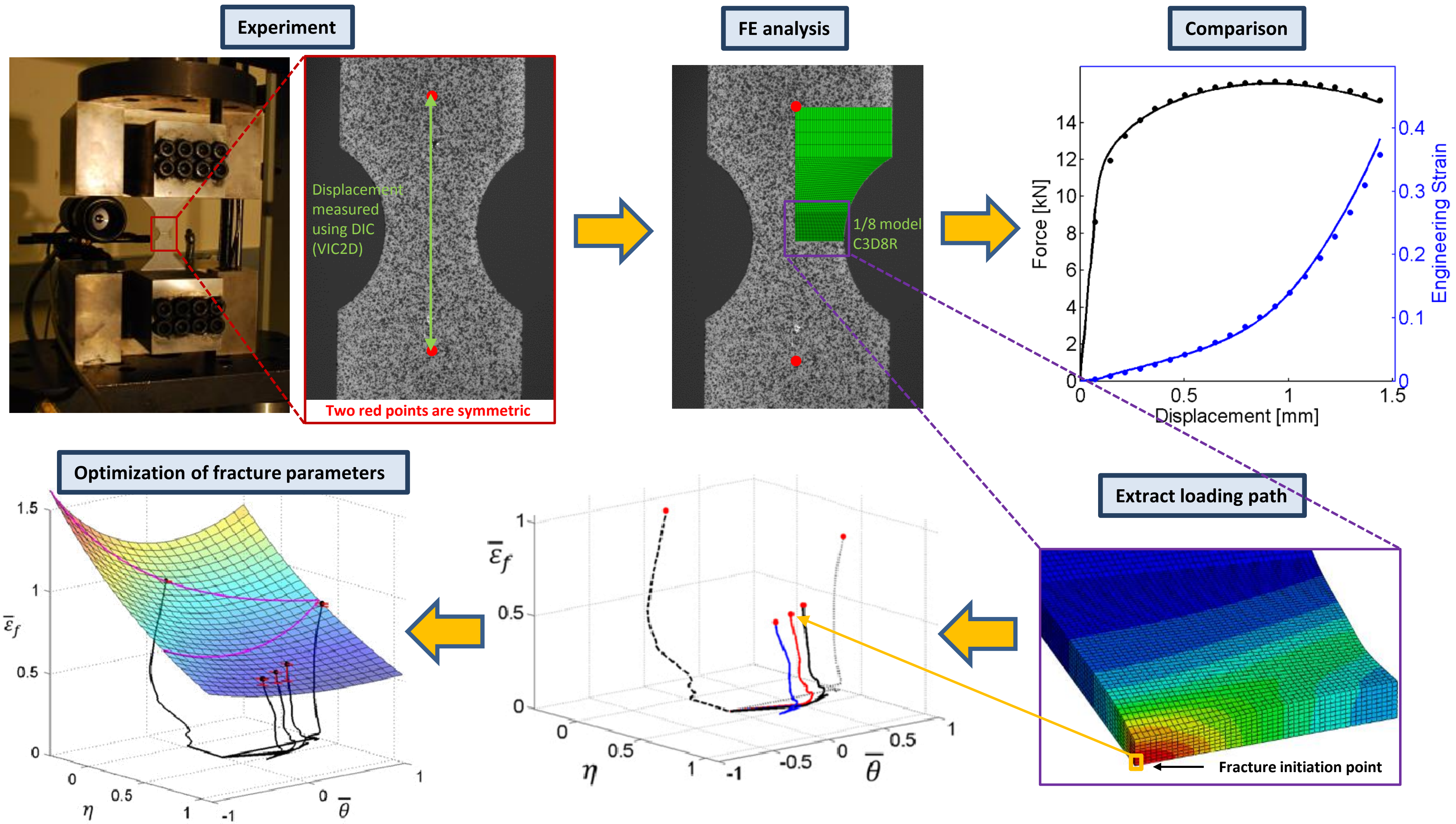

Extreme bending of riser with fracture